

Supporting information

Nanofibrous Hydrogel Composite Membrane with Ultrafast Transport Performance for Molecular Separation in Organic Solvents

Yi Li,^a Eric Wong,^b Alexander Volodine,^c Chris Van Haesendonck,^c Kaisong Zhang,^{*d} Bart Van der Bruggen,^{*a,e}

^a Department of Chemical Engineering, KU Leuven, Celestijnenlaan 200F, B-3001, Leuven, Belgium.

^b Department of Management and Technology, UC Leuven-Limburg, Herestraat 49, 3000, Leuven, Belgium

^c Department of Physics and Astronomy, KU Leuven, Celestijnenlaan 200 D, 3001 Leuven, Belgium

^d Key Laboratory of Urban Pollutant Conversion, Institute of Urban Environment, Chinese Academy of Sciences, 361021, Xiamen, PR China

^e Faculty of Engineering and the Built Environment, Tshwane University of Technology, Private Bag X680, Pretoria 0001, South Africa

* Corresponding authors.

E-mail address: bart.vanderbruggen@kuleuven.be (Bart Van der Bruggen); kszhang@iue.ac.cn (Kaisong Zhang).

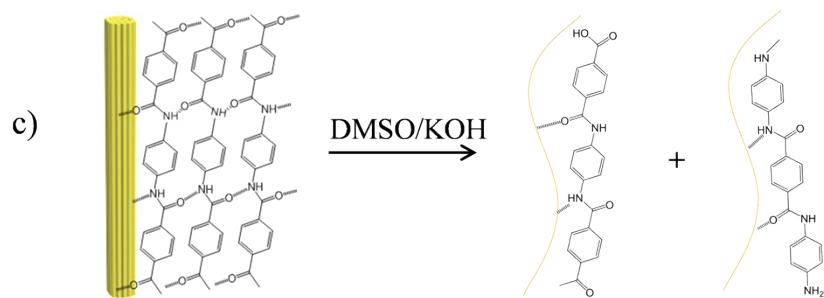
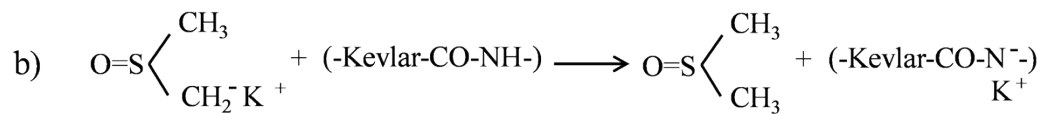
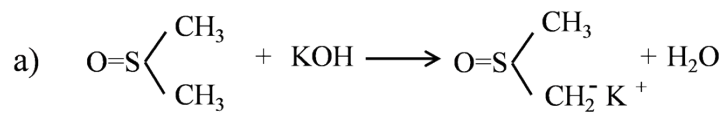


Fig. S1 (a- c) The assumed exfoliation process of Kevlar fiber in DMSO/KOH solution.

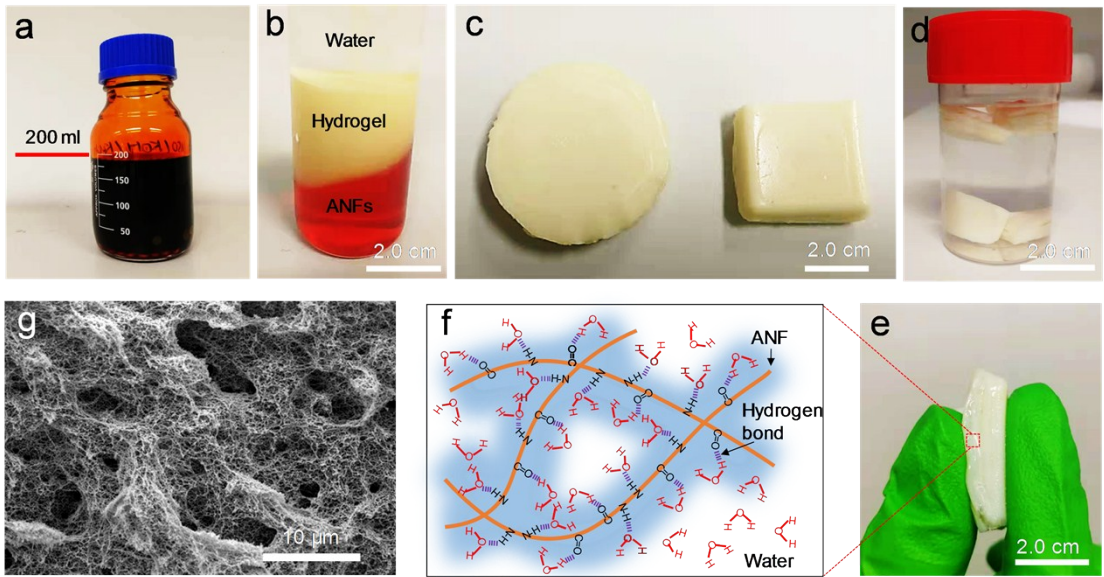


Fig. S2 The ANF hydrogel preparation process. (a) ANF dope solution (2.0 wt%). (b) The non-solvent induced phase separation process of ANFs dispersions in water. (c) The as-prepared hydrogels with different shapes. (d) The cut hydrogel cubic from a bulk hydrogel. (e) The hydrogel under compressing with fingers. (f) The interactions between water and ANFs. (g) The nanofibrous structure of ANF hydrogel.

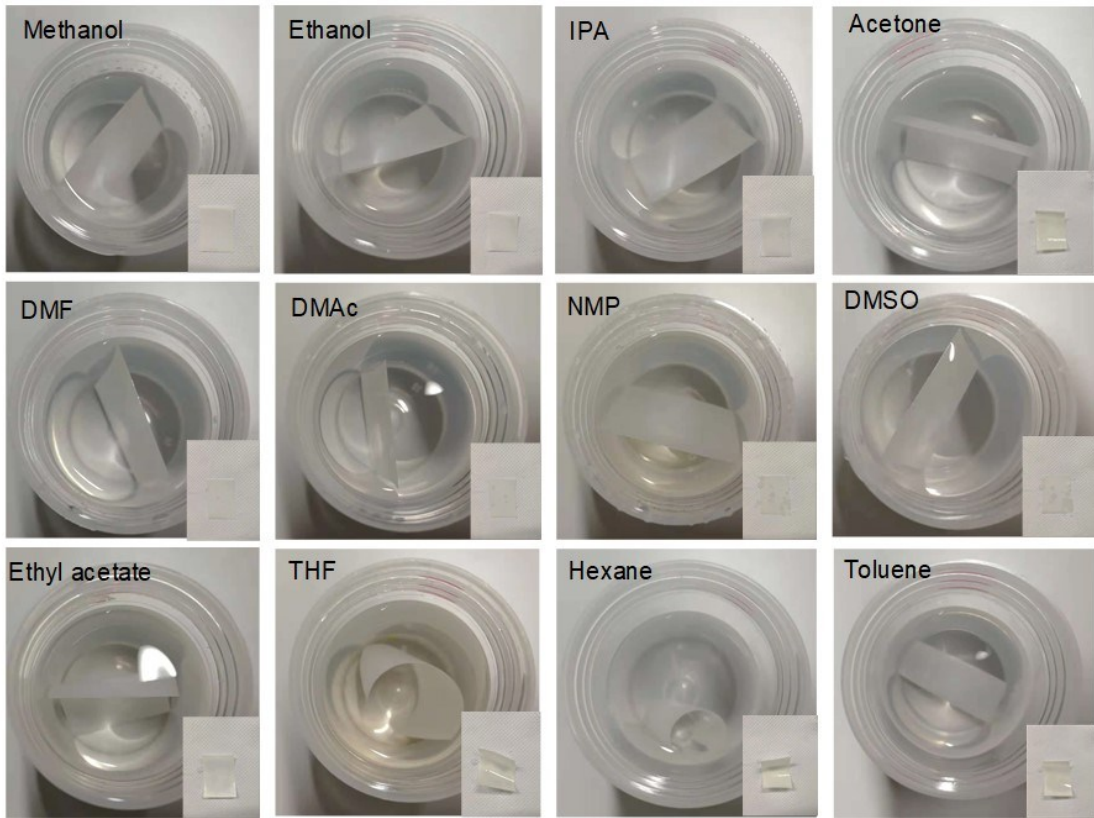


Fig. S3 The solvent resistance investigation of the ANF TFC membrane by immersing the membrane in different organic solvents. The membrane surface was examined after two weeks.

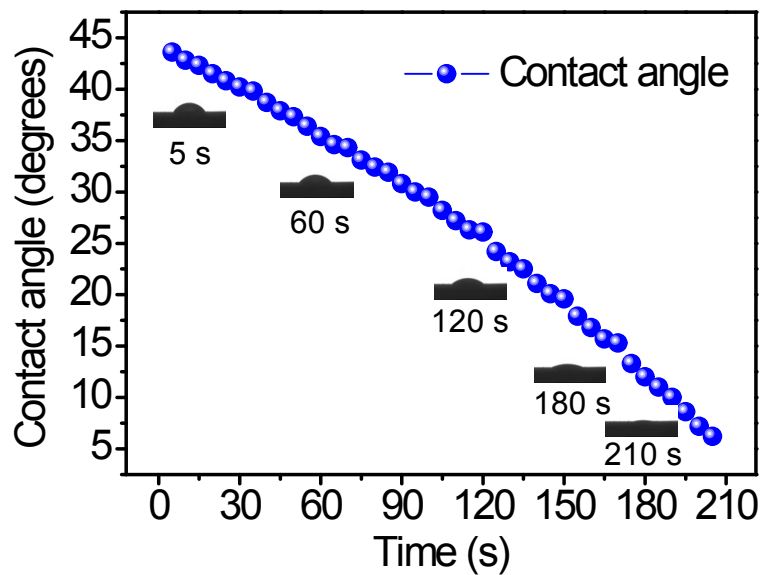


Fig. S4 Variations of water contact angle with time on ANF hydrogel substrate membrane surface.

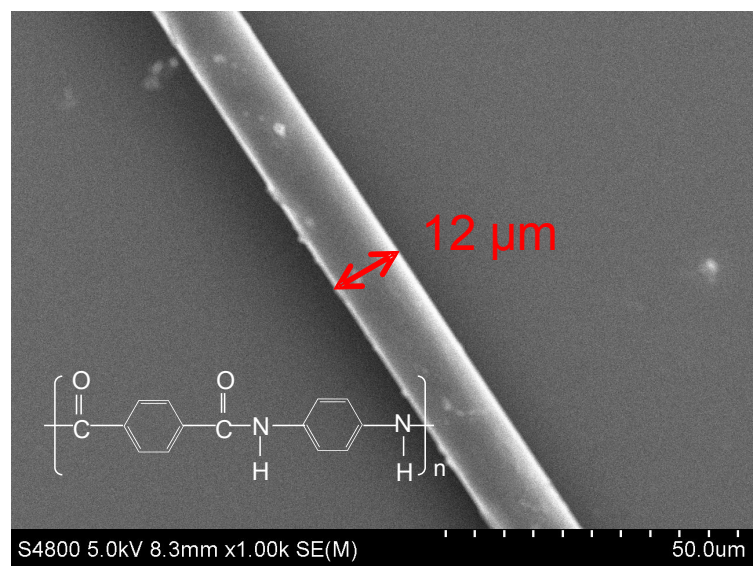


Fig. S5 SEM image of Kevlar fiber.

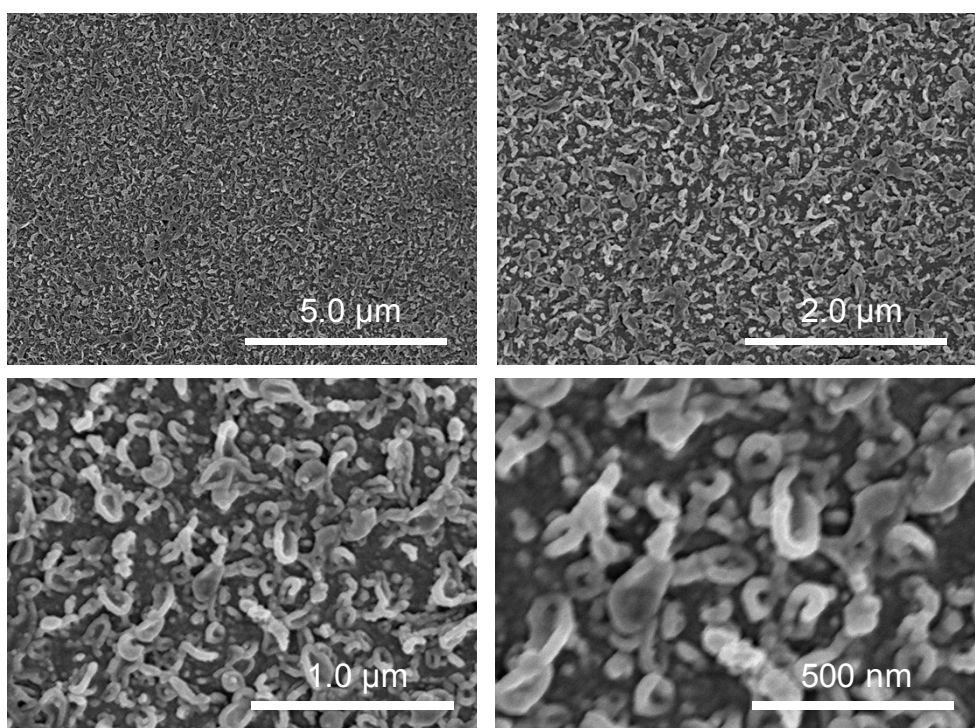
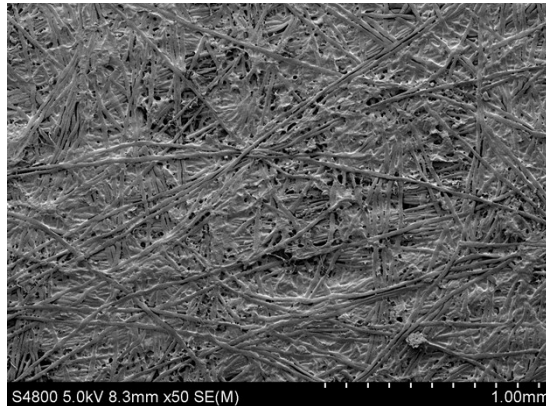
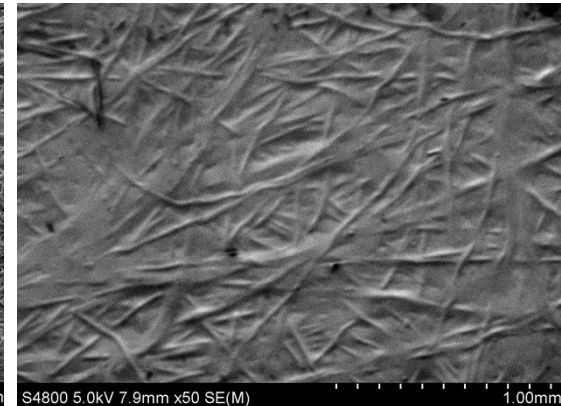


Fig. S6 The SEM images of the surface of the ANF TFC membrane in different magnifications.



S4800 5.0kV 8.3mm x50 SE(M)



S4800 5.0kV 7.9mm x50 SE(M)

Fig. S7 SEM image of the polyolefin (PO) non-woven fabric surface (left) and the ANF TFC membrane with the support of PO fabric.

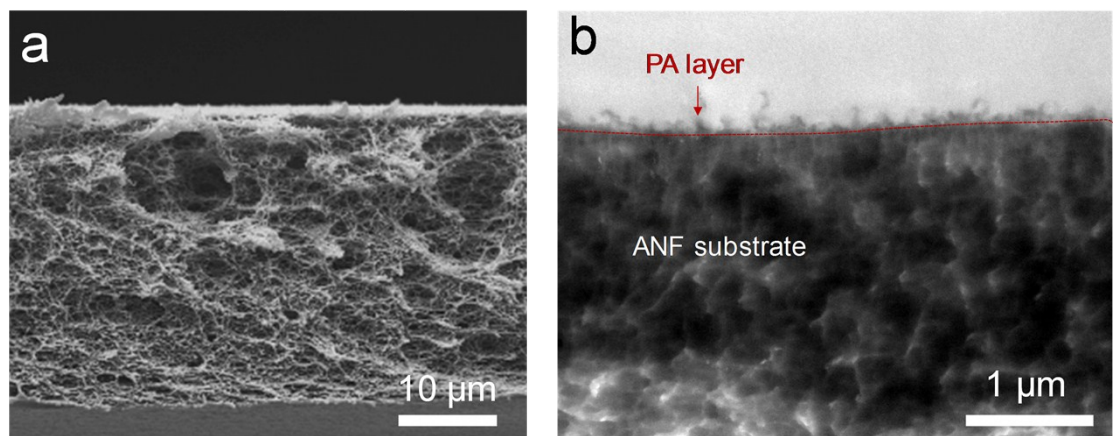


Fig. S8 (a) SEM image of the cross-section of the ANF hydrogel membrane without non-woven support. (b) TEM observation of the TFC membrane without DMF treatment.

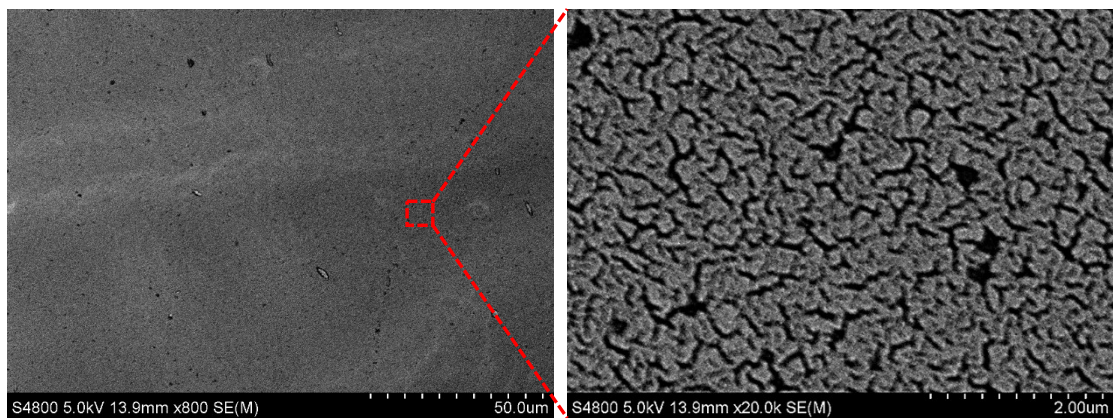


Fig. S9 SEM image of the ANF hydrogel surface on PP/PE non-woven fabric surface (left) and the surface with higher magnification (20,000 \times) (right).

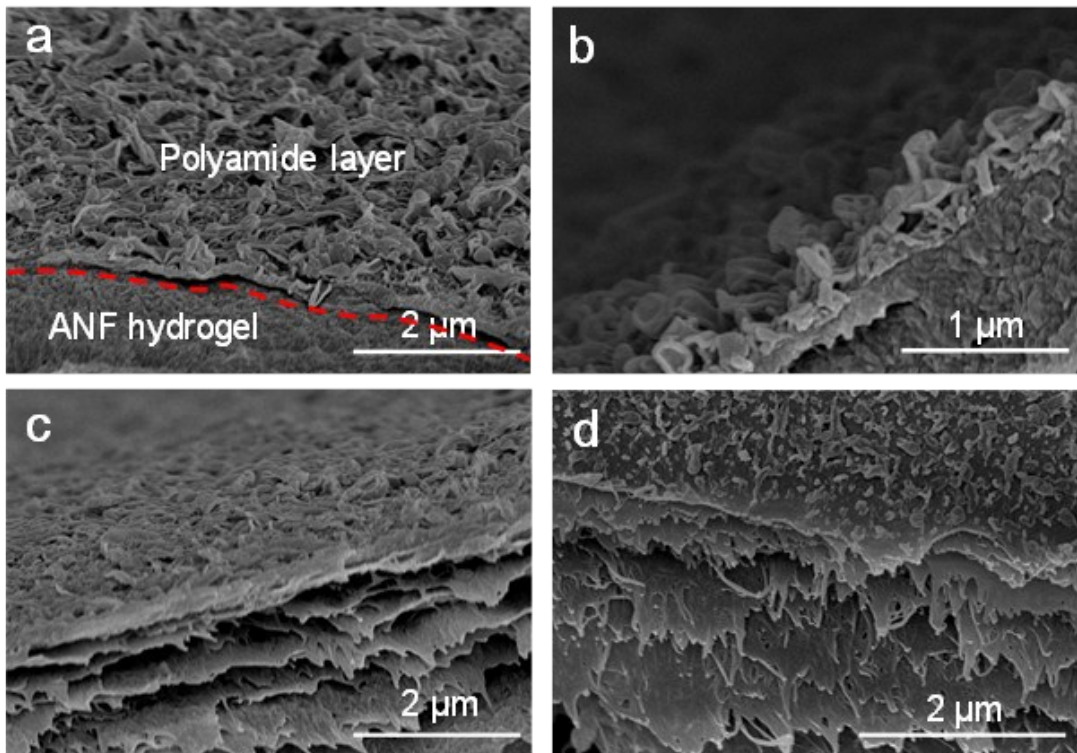


Fig. S10 (a, b) Cross sectional SEM images of the ANF TFC composite membrane without DMF treatment (The red dashed line showing the interface between polyamide layer and ANF hydrogel). (c, d) Cross-sectional SEM images of ANF TFC membrane with DMF treatment of 16 hours. (Membrane was dried with supercritical CO₂)

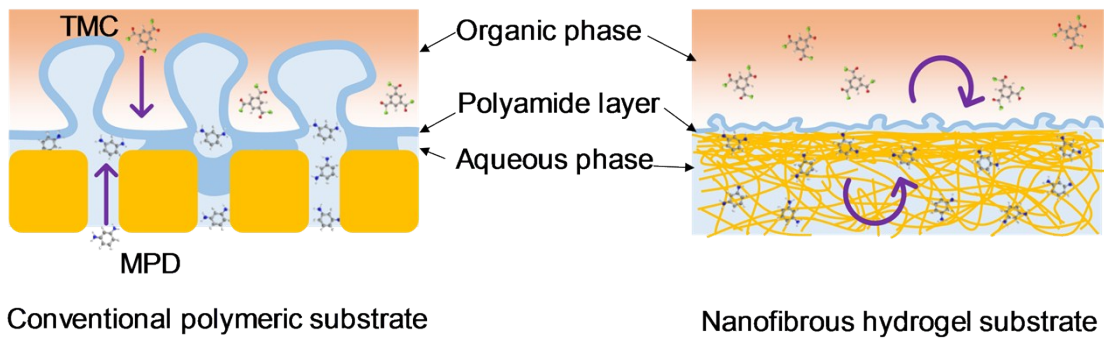


Fig. S11 Comparison of the interfacial polymerization on conventional polymeric substrate (Left) and nanofibrous hydrogel substrate (Right).

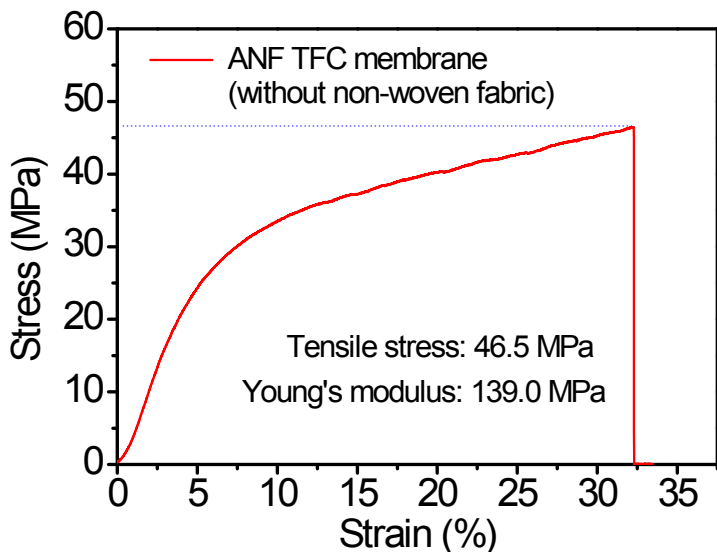


Fig. S12 Strain-stress curve of the dried ANF TFC membrane without the non-woven support.

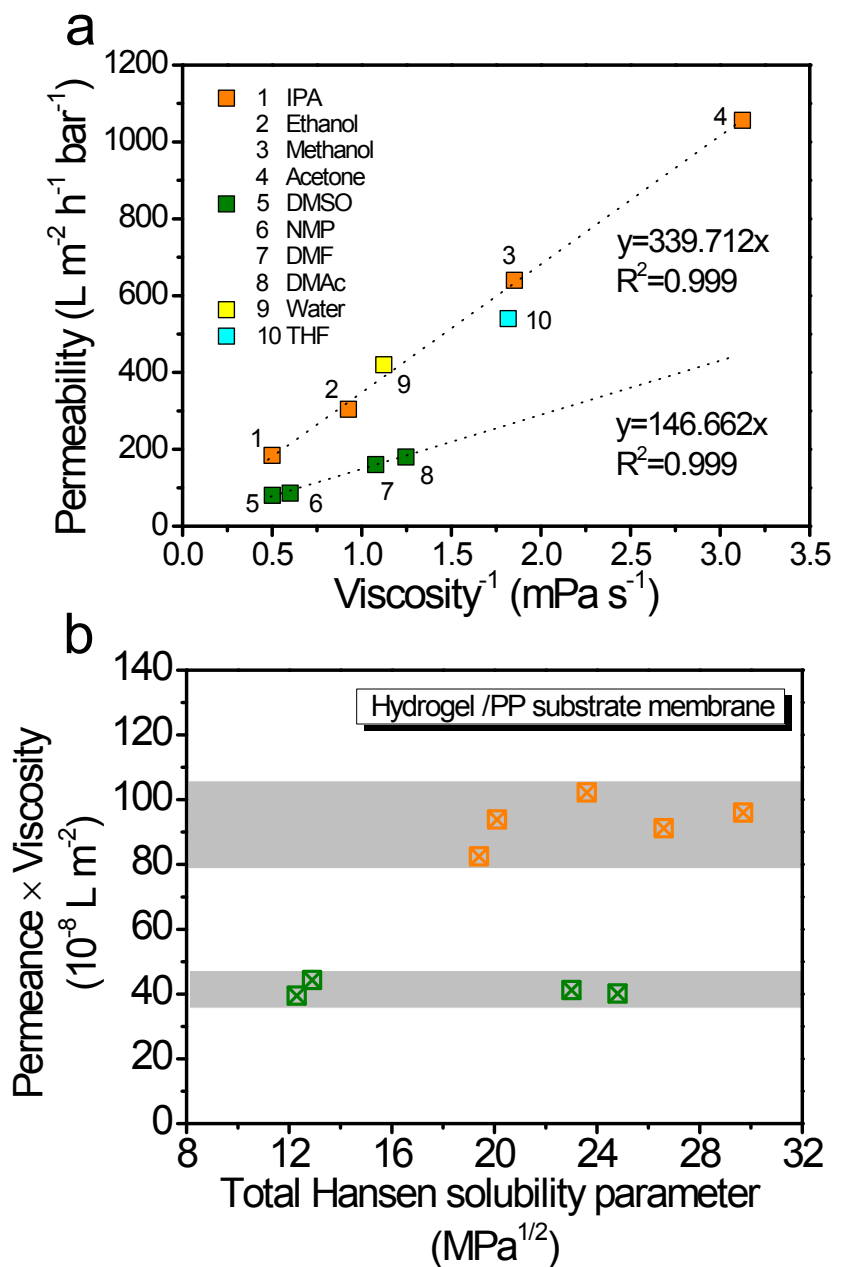


Fig. S13 (a) The transportation behavior of ANF hydrogel membrane against various solvents. (b) Product of permeance and viscosity of solvent as a function of the total Hansen solubility parameter for an ANF hydrogel membrane.

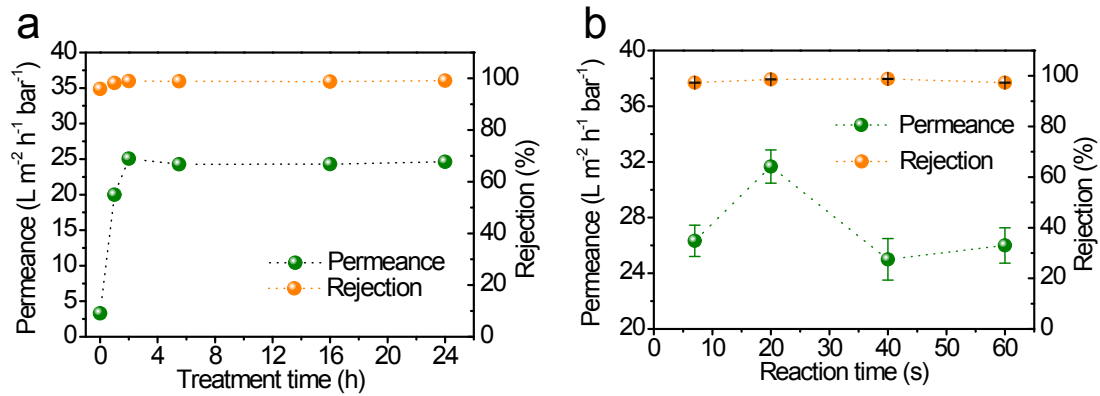


Fig. S14 Effect of DMF treatment time (a) and interfacial polymerization reaction time (b) on the separation performance of ANF TFC membrane. (Feed with the methanol/RB solution with dye concentration of 20 mg L⁻¹, tested at 4 bar, 500 rpm)

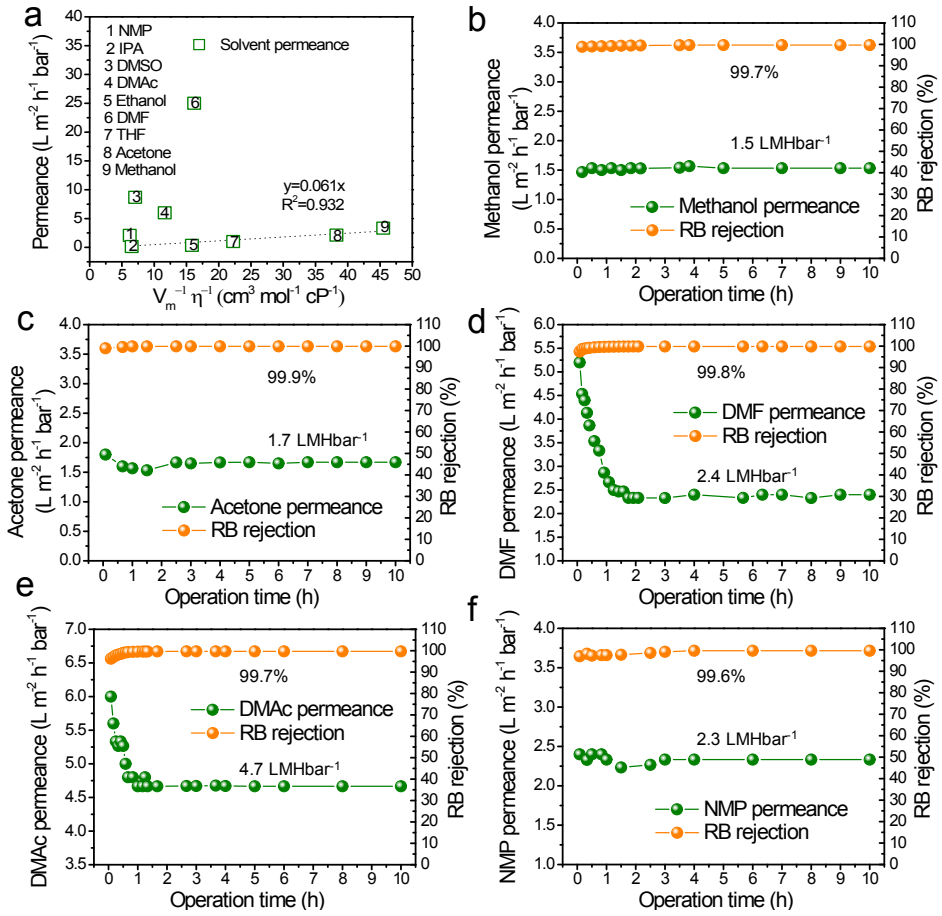


Fig. S15 (a) Pure solvent permeances against the combined solvent properties (solubility parameter, viscosity and mole volume) for ANF TFC membrane without DMF treatment. (b- f) Separation performance of ANF TFC membrane under solvent of (b) methanol, (c) acetone, (d) DMF, (e) DMAc and (f) NMP, respectively, with rose Bengal (1017 g mol^{-1}) concentration of 40 mg L^{-1} as the solute at 6 bar with stirring of 500 rpm.

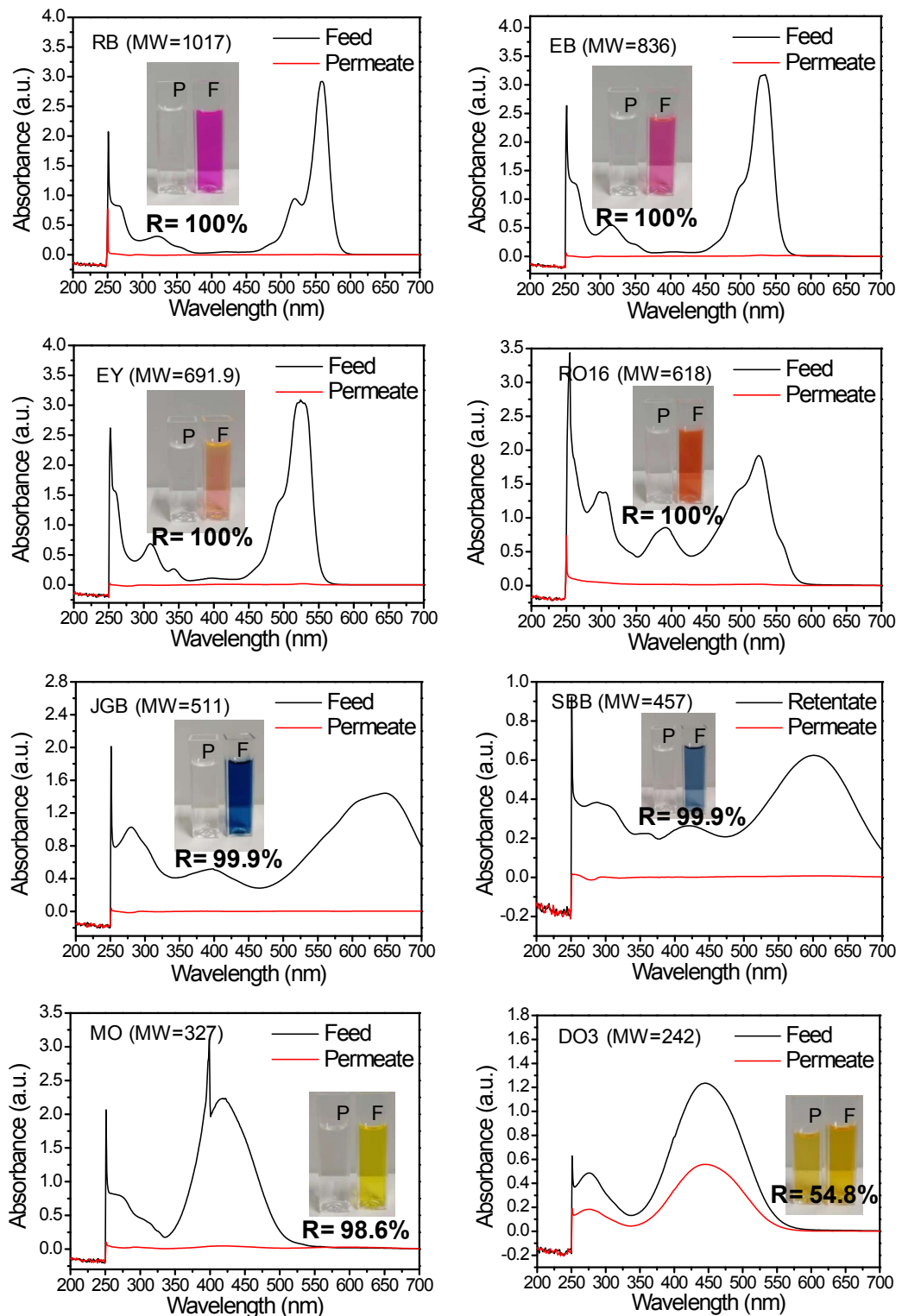


Fig. S16 Rejection of dyes with different molecular weight (M_w) for ANF TFC membrane. Inset photographs of the feed and permeate of dye/ethanol solution.

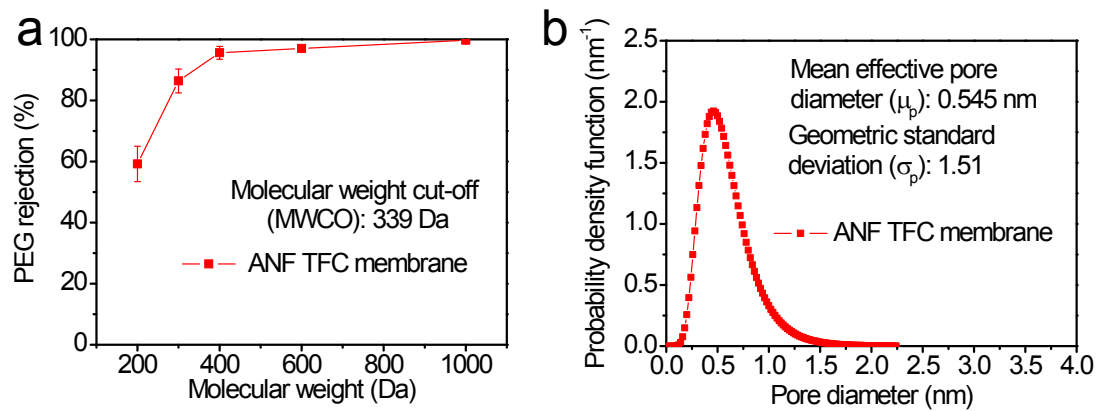


Fig. S17 (a) The rejection of PEGs with different molecular weights through ANF TFC membrane. (b) Probability density function curve of the ANF TFC membrane.

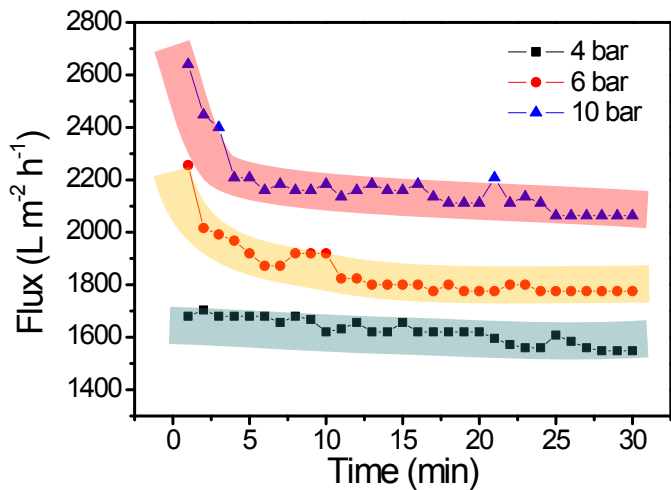


Fig. S18 Compaction of ANF hydrogel substrate tested with pure water at different pressures in the first half an hour.

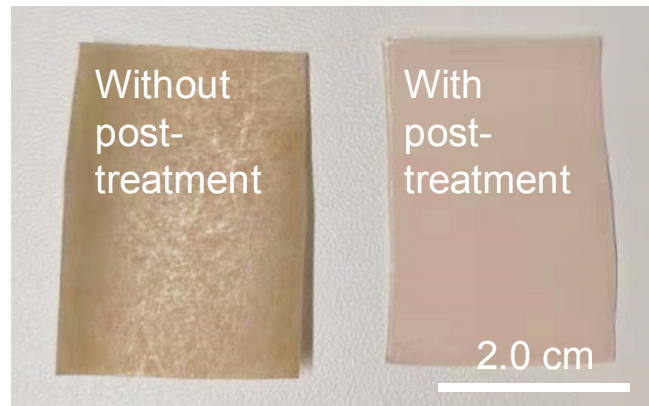


Fig. S19 Comparison of the ANF hydrogel TFC membrane without (Left) and with post-treatment (Right) after 180 d stored in a sealed bag. The membrane was treated with a mixture solution of isopropanol (IPA) and glycerol in a ratio of 7:3 (v/v) for one day.

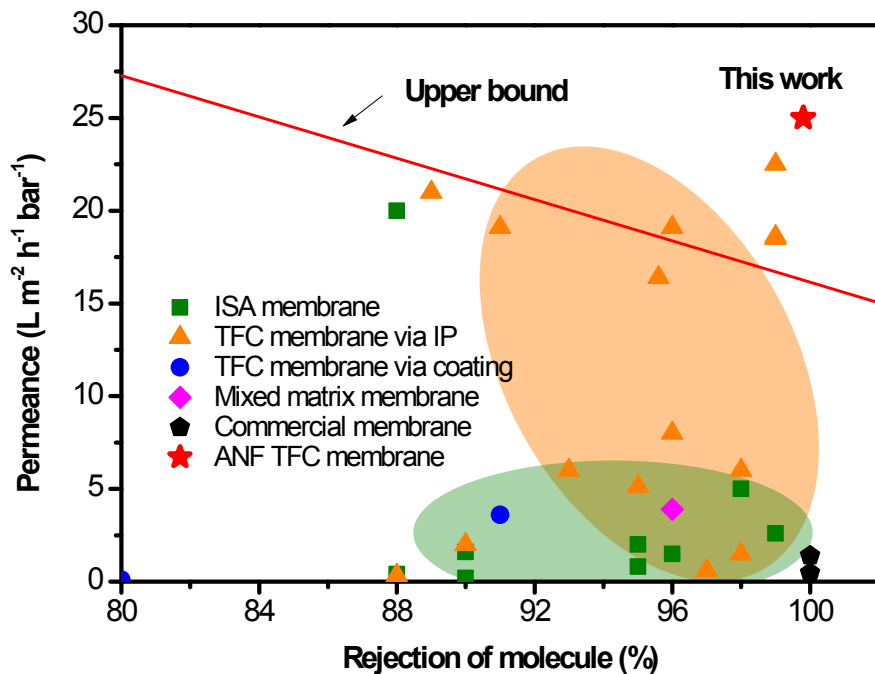


Fig. S20 Plot of permeance versus rejection of molecules, showing “trade-off” between permeance and selectivity. Typical OSN data of integral asymmetric (ISA) membrane, TFC membrane, mixed matrix membrane and commercial membrane were summarized from reported literature.

Table S1

Information of dyes used in this study.

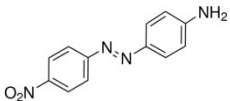
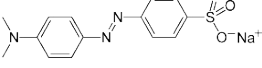
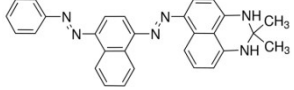
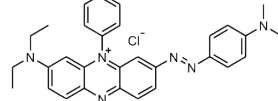
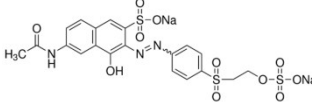
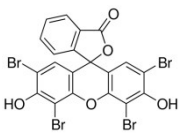
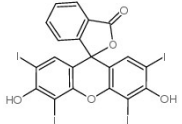
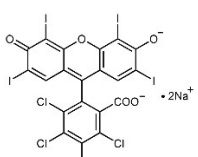
Dyes	Structure	Charge	Molecular weight (g mol ⁻¹)	Topological polar surface area (Å ²)	UV-vis absorption (nm)
Disperse Orange 3 (DO3)		0	242	96.6	$\lambda_{\text{EtOH}} = 445;$ $\lambda_{\text{EtOH}} = 418;$
Methyl Orange (MO)		-	327	93.5	$\lambda_{\text{DMF}}, \lambda_{\text{DMAc}} = 424;$ $\lambda_{\text{NMP}} = 430;$ $\lambda_{\text{water}} = 464;$
Sudan Black B (SBB)		0	457	73.5	$\lambda_{\text{EtOH}} = 606;$
Janus Green B (JGB)		+	511	48	$\lambda_{\text{EtOH}} = 651$
Reactive Orange 16 (RO16)		-	614	-	$\lambda_{\text{EtOH}} = 525;$ $\lambda_{\text{DMF}}, \lambda_{\text{NMP}} = 508;$ $\lambda_{\text{DMAc}} = 506;$
Eosin Y (EY)		0	648	76	$\lambda_{\text{EtOH}} = 528;$ $\lambda_{\text{EtOH}} = 530;$
Erythrosin B (EB)		0	836	76	$\lambda_{\text{DMF}} = 544;$ $\lambda_{\text{DMAc}} = 549;$ $\lambda_{\text{NMP}} = 541;$
Rose Bengal (RB)		-	1017	89.5	$\lambda_{\text{EtOH}}, \lambda_{\text{MeOH}}, \lambda_{\text{Acetone}} = 559;$ $\lambda_{\text{DMF}}, \lambda_{\text{DMAc}} = 564;$ $\lambda_{\text{NMP}} = 560;$

Table S2

Water content and swelling degree of the ANF hydrogel. (Size: 4 × 3 cm)

	Swelling degree	Water content (%)
	$(W_{wet} - W_{dry}) * W_{dry}^{-1}$ (g g ⁻¹)	$(W_{wet} - W_{dry}) * W_{wet}^{-1} * 100\%$
ANF hydrogel	2.5± 0.3	60.0± 3.8

Table S3

Solvent swelling degrees of ANF hydrogel membrane with PP/PE fabric in various organic solvents for two weeks.

Solvent	$(W_{wet} - W_{dry}) \cdot W_{dry}^{-1}$	$(W_{wet} - W_{dry}) \cdot W_{dry}^{-1} \cdot \text{density}^{-1} (\text{cm}^3 \text{ g}^{-1})$
Methanol	1.10	1.39
Ethanol	1.37	1.73
IPA	1.12	1.42
Acetone	0.19	0.24
Ethyl acetate	0.42	0.47
THF	1.26	1.42
DMF	1.68	1.78
DMAc	1.79	1.92
NMP	1.92	1.87
DMSO	2.08	1.89

Table S4

Physical properties of solvent used in this work.

Solvent	Molec ular weight (Mw, g mol ⁻¹)	Dens ity (g cm ⁻³)	Surface tension (γ, mN m ⁻¹ , 20 °C)	Visco sity (η, cP, 20 °C)	Relati ve permittiv ity (g)	Mole volum e (V _m , cm ³ mol ⁻¹) ^a	Hansen solubility parameter			
							δ _d (MPa ^{1/2}) ^a	δ _p (MPa ^{1/2}) ^a	δ _h (MPa ^{1/2}) ^a	δ _{sp} (MPa ^{1/2}) ^b
Methanol	32.0	0.79	22.7	0.59	32.7	40.7	15.1	12.3	22.3	29.6
Ethanol	46.1	0.79	22.1	1.2	24.5	58.5	15.8	8.8	19.4	26.5
IPA	60.1	0.79	23.0	2.4	19.9	76.8	15.8	6.1	16.4	23.6
Acetone	58.1	0.79	25.2	0.32	20.7	74.0	15.5	10.4	7.0	20.0
NMP	99.1	1.03	40.8	1.67	32.2	96.5	18.0	12.3	7.2	23.0
DMAc	87.1	0.94	36.7	2.14	37.8	92.5	16.8	11.5	10.2	22.8
DMF	73.1	0.94	37.1	0.92	36.7	77.0	17.4	13.7	11.3	24.8
DMSO	78.1	1.10	43.5	2.24	46.7	71.3	18.4	16.4	10.2	26.7
EtOAc	88.1	0.90	24.0	0.46	6.0	98.5	15.8	5.3	7.2	18.2
THF	72.1	0.89	26.4	0.55	7.6	81.7	16.8	5.7	8.0	19.5
Hexane	86.2	0.66	18.4	0.31	1.9	131.6	14.9	0	0	14.9
Water	18.0	1.00	72.8	1.0	78.5	18.0	15.5	16.0	42.3	47.8

^a Data were obtained from the book “Hansen Solubility Parameters: A User’s Handbook (second edition)”. Hansen Solubility Parameters, HSP, δ_d for Dispersion (van der Waals), δ_p for Polarity (related to dipole moment) and δ_h for hydrogen bonding.

^b Data were calculated from the Hansen solubility parameters.

Table S5

Comparison of OSN performance in harsh organic solvent for nanofibrous hydrogel TFC membrane in this work with other polymer substrate based TFC membrane via interfacial polymerization.

Materials	Solvent	Permeance (L m ⁻² h ⁻¹ bar ⁻¹)	Solute (g mol ⁻¹)	Rejection (%)	Ref.
PA/PI	Acetone	2.4	Styrene oligomers (236- 1200 g mol ⁻¹)	95.0 (236 g mol ⁻¹)	[1]
	DMF	1.5		91.0 (236 g mol ⁻¹)	
PA/PI	DMF	3.9	Tetracycline (444 g mol ⁻¹)	95.0	[2]
(PA-COF)/PI	DMF	5.5	Rose Bengal (1017 g mol ⁻¹)	99.5	[3]
(DA/TMC)/PI	DMF	1.15	Rose Bengal (1017 g mol ⁻¹)	99.9	[4]
(PAR-BHPF)/PI	Acetone	8.4	Styrene oligomers (236- 1200 g mol ⁻¹)	97.0 (236 g mol ⁻¹)	[5]
PA/PAN	Acetone	6.0	Oleic acid (282 g mol ⁻¹)	92.0	[6]
(Morin-TPC)/PAN	NMP	0.3	Brilliant Blue (826 g mol ⁻¹)	96.0	[7]
PA/PBOI	DMF	7.7	Styrene oligomers (236- 1200 g mol ⁻¹)	>90.0 (600 g mol ⁻¹)	[8]
(Tannic acid-TPC)/PAN	NMP	0.08	Brilliant Blue (826 g mol ⁻¹)	95.0	[9]
PA/Cellulose	DMF	1.4	Amido-Black (617 g mol ⁻¹)	92.0	[10]
PA/ANF hydrogel (without solvent treatment)	DMF	20.3	Methyl orange (327 g mol ⁻¹)	64.0	This work
		10.6	Reactive orange 16 (618 g mol ⁻¹)	92.3	
		8.1	Erythrosin B (836 g mol ⁻¹)	99.3	

		3.5	Rose Bengal (1017 g mol ⁻¹)	99.4	
DMAc	8.4	Methyl orange (327 g mol ⁻¹)	91.4	This work	
		Reactive orange			
	7.6	16 (618 g mol ⁻¹)	93.0		
	7.3	Erythrosin B (836g mol ⁻¹)	97.1		
NMP	5.3	Rose Bengal (1017 g mol ⁻¹)	99.7		
	4.9	Methyl orange (327 g mol ⁻¹)	94.4	This work	
		Reactive orange			
	8.8	16 (618 g mol ⁻¹)	93.1		
	1.8	Erythrosin B (836g mol ⁻¹)	99.9		
	2.3	Rose Bengal (1017 g mol ⁻¹)	99.6		
PA/ANF hydrogel (with solvent treatment)	Acetone	19.0	Rose Bengal (1017 g mol ⁻¹)	100.0	This work
	DMF	6.0		99.5	This work
	DMAc	10.0		97.0	This work
	NMP	5.0		100.0	This work

- [1] M. F. Jimenez Solomon, Y. Bhole, A. G. Livingston, *J. Membr. Sci.* **2013**, 434, 193.
- [2] S. P. Sun, T. S. Chung, K. J. Lu, S. Y. Chan, *AIChE J.* **2014**, 60, 3623.
- [3] C. Li, S. Li, L. Tian, J. Zhang, B. Su, M. Z. Hu, *J. Membr. Sci.* **2019**, 572, 520.
- [4] C. Li, S. Li, L. Lv, B. Su, M. Z. Hu, *J. Membr. Sci.* **2018**, 564, 10.
- [5] M. F. Jimenez-Solomon, Q. Song, K. E. Jelfs, M. Munoz-Ibanez, A. G. Livingston, *Nat. Mater.* **2016**, 15, 760.
- [6] I. C. Kim, J. Jegal, K. H. Lee, *J. Polym. Sci., Part B: Polym. Phys.* **2002**, 40, 2151.
- [7] L. Pérez Manríquez, P. Neelakanda, K. V. Peinemann, *J. Membr. Sci.* **2018**, 554, 1.
- [8] J. H. Kim, S. J. Moon, S. H. Park, M. Cook, A. G. Livingston, Y. M. Lee, *J. Membr. Sci.* **2018**, 550, 322.
- [9] L. Pérez Manríquez, P. Neelakanda, K. V. Peinemann, *J. Membr. Sci.* **2017**, 541, 137.
- [10] M. H. Abdellah, L. Pérez Manríquez, T. Puspasari, C. A. Scholes, S. E. Kentish, K. V. Peinemann, *J. Membr. Sci.* **2018**, 567, 139.